

Cite this: *Phys. Chem. Chem. Phys.*, 2011, **13**, 9676–9684

www.rsc.org/pccp

PAPER

Five isomers of monomeric cytosine and their interconversions induced by tunable UV laser light†

Leszek Lapinski,^a Igor Reva,^b Maciej J. Nowak^{*a} and Rui Fausto^b

Received 7th December 2010, Accepted 10th March 2011

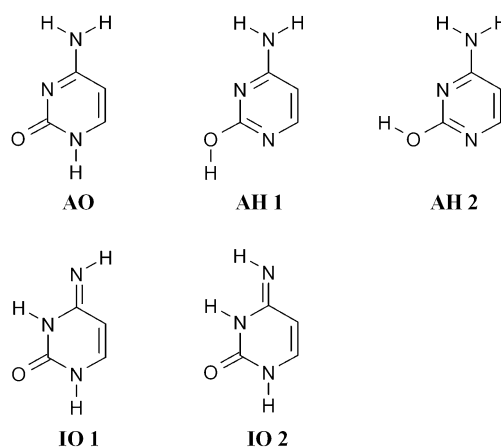
DOI: 10.1039/c0cp02812f

Photoisomerization processes involving five isomers of cytosine were induced by narrowband tunable UV irradiation of matrix-isolated monomers of the compound. Irradiation of an argon matrix containing cytosine monomers with UV $\lambda = 313$ nm laser light resulted in *syn* \leftrightarrow *anti* photoisomerizations between the two imino–oxo forms, whereas the substantially more populated amino–hydroxy and amino–oxo forms stayed intact. Subsequent irradiation with shorter-wavelength UV $\lambda = 311$ nm laser light led to two concomitant phototautomeric processes consuming the amino–oxo isomer: (i) an oxo \rightarrow hydroxy hydrogen-atom transfer photoprocess converting the amino–oxo form into the amino–hydroxy tautomer; (ii) amino \rightarrow imino hydrogen-atom transfer converting the amino–oxo form into the imino–oxo isomers. The UV-induced phototransformations, together with mutual conversions of the two amino–hydroxy conformers induced by irradiation with narrowband NIR light, allowed positive detection and identification of the five isomeric forms of monomeric cytosine. This is the first experimental observation of all five low-energy isomers of cytosine.

1. Introduction

In the recent decade, photophysics of cytosine monomers in the gas phase was intensively studied using modern experimental^{1,2} as well as theoretical³ methods. Experimental investigations on picosecond and subpicosecond excited-state dynamics revealed multiexponential decay following the UV excitation of cytosine. Two dominating components of this decay are characterized by subpicosecond 160 fs and picosecond 1.9 ps lifetimes.¹ Several mechanisms of the ultrafast decay of electronically excited cytosine were conceived³ and supported by the state-of-the-art calculations of excited-state potential energy surfaces. The general picture of very effective intramolecular quenching of the cytosine excited state(s), prohibiting formation of structurally modified photoproducts, stems from both experimental and theoretical works. In line with these conclusions, no products of unimolecular photochemistry of cytosine were proposed. Moreover, the question of the structure, actually adopted by cytosine molecules in the gas phase prior to any excitation, was mostly disregarded in these studies.

On the other hand, numerous theoretical *ab initio* calculations on relative energies of cytosine tautomers were carried out in recent years. The results of the contemporary quantum chemical calculations^{4,5} predict a consistent (and probably correct) energy ordering of cytosine isomers. According to these calculations, carried out at the CCSD(T) or QCISD(T) levels, the most stable tautomer of monomeric cytosine should be the amino–hydroxy (AH) form. Of the two AH conformers (differing by rotation of the hydroxyl group by *ca.* 180°, see Scheme 1), AH1 was theoretically predicted to be more stable by 2.9–3.1 kJ mol⁻¹ than AH2. The energy of the amino–oxo (AO) form was theoretically computed to be higher by 4.9–6.3 kJ mol⁻¹ than



Scheme 1 Structures of the lowest-energy isomeric forms of cytosine.

^a Institute of Physics, Polish Academy of Sciences, Al. Lotnikow 32/46, 02-668 Warsaw, Poland. E-mail: mnowak@ifpan.edu.pl

^b Department of Chemistry, University of Coimbra, 3004-535 Coimbra, Portugal

† Electronic supplementary information (ESI) available: The effects of irradiation of matrix-isolated cytosine with NIR and UV ($\lambda = 300$ nm) light (Fig. S1 and S2); spectral indications of the AO \rightarrow AH phototautomeric reaction (Fig. S3); assignment of the observed IR bands to AH1, AH2, AO, IO1 or IO2 forms (Fig. S4 and Table S1); IR bands due to IO2 form growing upon UV ($\lambda = 300$ nm) irradiation (Fig. S5). See DOI: 10.1039/c0cp02812f

the energy of the most stable **AH1** isomer. As far as the imino–oxo forms are concerned, the relative energies of **IO1** and **IO2** should be *ca.* 7 and 12 kJ mol⁻¹, with respect to **AH1**. Hence, for cytosine in the gas phase, together with the dominating **AH1** and **AH2** isomers, also **AO** and **IO1** forms should be significantly populated. The relative population of **IO2** should be much lower, and all the remaining forms of cytosine (whose relative energies are much higher) should not be populated at all.

Experimental studies on relative populations of cytosine isomers in the gas phase are by far less abundant. The most populated **AH** and **AO** forms were experimentally found using microwave⁶ and photoelectron⁷ techniques. Forms **AH1**, **AH2** and **AO** were identified for cytosine monomers trapped in helium nanodroplets at 0.37 K.⁸ So far, no unquestionable experimental evidence of the imino–oxo **IO** forms of gaseous cytosine has been provided.

As revealed by previous investigations,^{9,10} monomers of cytosine, in different isomeric forms, can be effectively trapped from the gas phase into low-temperature matrices. In our recent study,⁹ matrix-isolated cytosine was irradiated with narrowband near infrared (NIR) light. The dominating amino–hydroxy **AH1** and **AH2** isomers were found to convert into each other upon NIR irradiation at 7013 or at 7034 cm⁻¹. On the basis of this effect, two sets of IR bands were assigned to **AH1** and **AH2**. Together with the IR spectral features attributed to **AH1** and **AH2**, a set of bands not affected by any NIR irradiation was observed. This demonstrated that, alongside **AH1** and **AH2**, other isomers of cytosine were trapped in solid argon.

Effects of UV irradiation can be used to differentiate between the isomeric forms of cytosine codeposited in the same matrix. In previous investigations,^{10,11} monomers of cytosine isolated in Ar or N₂ matrices were irradiated with broadband UV light. High-pressure xenon or mercury lamps, fitted with appropriate cutoff filters, were used for this purpose. This approach allowed unequivocal identification of **AH** and **AO** forms of matrix-isolated cytosine. However, the intrinsic limitations of broadband UV irradiation did not allow a very detailed analysis of the observed photoeffects. In particular, it was not possible to separately observe the photoreactions of the minor **IO** forms of the compound.

In the current study, matrix-isolated cytosine monomers were excited at a series of chosen wavelengths using tunable, narrowband UV laser light. Such an approach permitted us to obtain a much clearer picture of the UV-induced transformations of monomeric cytosine, including separate observation of phototransformations of **IO** and **AO** forms. This, in turn, allowed a significantly more conclusive analysis of the experimental results, with special emphasis devoted to the photochemistry of the minor, imino–oxo **IO** forms.

2. Methods

2.1 Experimental section

The crystalline sample of cytosine (purity 99%) used in the present study was a commercial product supplied by Sigma. In order to prepare Ar matrices containing isolated monomers

of cytosine, a solid sample of the compound was heated (to *ca.* 495 K) in a miniature glass oven placed in the vacuum chamber of a helium-cooled cryostat. Similarly to the previous studies,^{6,10,11} no signs of thermal decomposition were observed for cytosine sublimating at 495 K. Vapors of cytosine were deposited together with large excess of argon (purity N6.0, supplied by Air Liquide) onto a CsI window cooled to 12 K. The IR spectra were recorded in the 4000–400 cm⁻¹ range, with 0.5 cm⁻¹ resolution, using a Thermo Nicolet 670 FTIR spectrometer equipped with a KBr beam splitter and a DTGS detector. Matrices were irradiated with the frequency doubled signal beam of the Quanta-Ray MOPO-SL pulsed (10 ns) optical parametric oscillator (FWHM \approx 0.2 cm⁻¹, repetition rate 10 Hz, pulse energy \approx 1.0 mJ) pumped with a pulsed Nd:YAG laser.

2.2 Computational section

The geometries of the five lowest-energy isomeric forms of cytosine (see the structures presented in Scheme 1) were fully optimized using the density functional method DFT(B3LYP) with Becke's three-parameter exchange functional¹² and the Lee, Yang, Parr correlation functional.¹³ The 6-31++G(d,p) basis set was applied in these calculations. At the optimized geometries, the harmonic vibrational frequencies and IR intensities were calculated at the same DFT(B3LYP)/6-31++G(d,p) level. The computed harmonic vibrational wavenumbers were scaled down by a single factor of 0.978. All the calculations were performed with the Gaussian 03 program.¹⁴

3. Results and discussion

Monomers of cytosine were deposited into low-temperature Ar matrices. The infrared spectra of these matrices were virtually the same as those recorded in the previous works.^{10,11} The quality of the spectra obtained in the current experiments was somewhat better, due to the higher sensitivity and resolution of the used spectrometer.

In the present work, matrix-isolated cytosine was irradiated with UV light of a frequency doubled signal beam of the optical parametric oscillator (FWHM \approx 0.2 cm⁻¹). The preliminary choice of wavelengths of the applied UV light was guided by the absorption spectra of isolated cytosine monomers, recorded by Nir *et al.*¹⁵ using the REMPI technique. In the long wavelength region of the REMPI spectra, medium-strong absorptions were observed at 313–314 nm. These absorptions were assigned to **AO** form of the compound. At longer wavelengths (315–316 nm) only significantly weaker bands were found. Those bands were tentatively assigned to other isomers, probably to **IO**. Absorptions due to the **AH** tautomer appeared at much shorter wavelengths (*ca.* 275 nm).

3.1 *Syn* \leftrightarrow *anti* photoisomerization in the imino–oxo forms

The UV irradiations of matrix-isolated cytosine carried out in the present study started at wavelength 320 nm. After each irradiation the sample was monitored by recording an infrared spectrum. No photoreactions occurred in matrices irradiated at wavelengths 320–316 nm. The first phototransformations were observed for $\lambda = 314$ nm, though the effects of irradiation at this wavelength were very slight. More pronounced

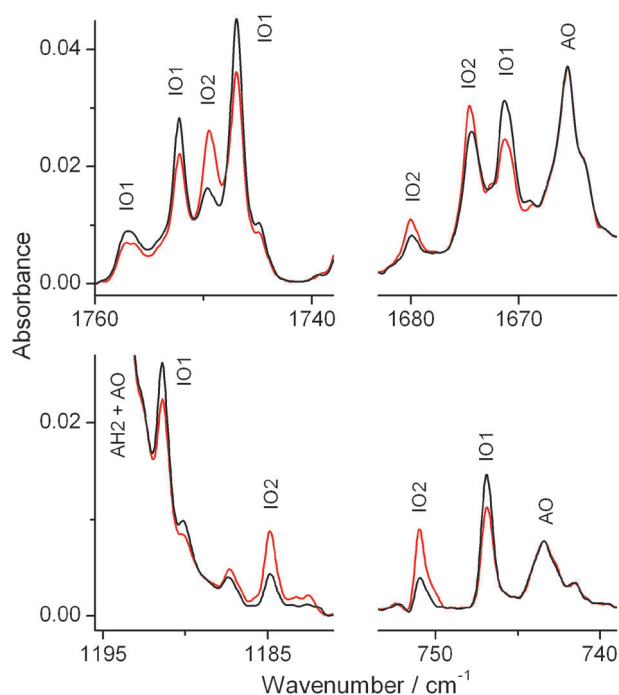
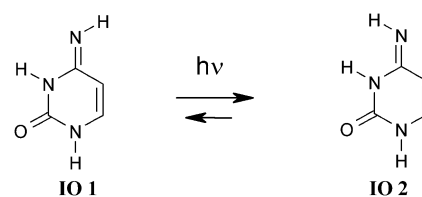


Fig. 1 *Syn* ↔ *anti* isomerization of the imino–oxo forms of cytosine induced by UV ($\lambda = 312$ nm) irradiation with monochromatic laser light. Fragments of the infrared spectrum of cytosine monomers isolated in an Ar matrix: (black) recorded after deposition of the matrix; (red) recorded after irradiation at 312 nm.

changes in the IR spectra occurred upon irradiation at 313 and 312 nm. The changes induced by irradiations at 313 and 312 nm concerned only two sets of low- or very low-intensity bands. All of those bands were already affected by UV ($\lambda = 314$ nm) light. Upon irradiations at 314, 313 or 312 nm, one set of bands decreased in intensity, whereas the intensities of the bands belonging to the other set increased (see Fig. 1). On the other hand, irradiations at these wavelengths did not affect any intense bands in the IR spectrum. This indicated that the substrate of the photoreaction as well as the photoproduct must be minor isomers of cytosine. The obvious candidates for these isomers are the imino–oxo **IO1** and **IO2** forms.

Taking into account the theoretically predicted relative energies of the imino–oxo forms, **IO1** should be significantly more populated than **IO2** in a matrix before any irradiation.^{5,16} Because the form being consumed upon UV ($\lambda = 314$, 313 or 312 nm) irradiation is more populated in a freshly deposited matrix, it can be tentatively assigned to **IO1**. Consequently, the form being photoproducted upon such irradiation can be assigned to **IO2**. The photoreaction transforming one of the imino–oxo forms into the other is a *syn* ↔ *anti* photoisomerization or, in other words, a flip of the hydrogen atom of the imino group (see Scheme 2). A similar photoisomerization reaction was previously observed for the imino–oxo isomers of matrix-isolated 1-methylcytosine.¹⁷

The positions of the IR bands in the spectrum of the substrate and of the product of the photoreaction induced by irradiation of cytosine at 314, 313 or 312 nm confirm the above interpretation. In the 1800–1600 cm^{-1} spectral range, where the bands due to stretching vibrations of the C=O,



Scheme 2 UV-induced isomerization transforming one of the imino–oxo forms of cytosine into the other.

C=N and C=C double bonds can be expected, the IR absorptions decreasing upon UV ($\lambda = 314$, 313 or 312 nm) irradiations appear at 1757/1752/1747 and at 1671 cm^{-1} , whereas those increasing in intensity were found at 1750 and 1675 cm^{-1} . In the spectra of both forms involved in the observed photoconversion, the bands at ~ 1750 cm^{-1} should originate from the stretching vibrations of the carbonyl group ($\nu\text{C}=\text{O}$). Such a wavenumber is higher by ~ 30 cm^{-1} than that of the IR band due to the $\nu\text{C}=\text{O}$ vibration in the **AO** form of cytosine. In the experimental IR spectrum, this last band was found at 1720/1717 cm^{-1} . The bands due to $\nu\text{C}=\text{O}$ vibrations were theoretically predicted at 1762, 1758 and 1735 cm^{-1} for **IO1**, **IO2** and **AO**, respectively. Hence, according to the calculations, the $\nu\text{C}=\text{O}$ bands in the spectra of **IO1** and **IO2** should partly overlap and should appear at wavenumbers higher by some 25 cm^{-1} , with respect to the $\nu\text{C}=\text{O}$ band of **AO**. This theoretical prediction is in agreement with the experimental picture and supports the assignment of **IO1** and **IO2** to the forms involved in the photoconversion induced by UV irradiation at 314–312 nm.

The low-intensity bands increasing or decreasing upon irradiation at 314–312 nm were observed throughout the whole IR spectrum of cytosine. Many of them overlap with much stronger bands of **AH** and **AO** forms. The clearly observed spectral features of the **IO1** reactant were found at 1757/1752/1747, 1671, 1472, 1191, 1124, 818, 747 and 636 cm^{-1} . The bands due to the **IO2** product were detected at 1750, 1680, 1675, 1463/1459, 1416, 1390, 1276/1275/1271, 1185, 1057, 780/779, 751, 686 and 584 cm^{-1} . Representative examples of IR bands belonging to these two sets are shown in Fig. 1.

Note also that upon irradiation at 314–312 nm the **IO1** substrate could not be totally converted into the **IO2** product; irradiations at these wavelengths were leading always to photostationary states. At any of such photostationary states, the population ratio of **IO1** and **IO2** was found to be dependent on the wavelength of UV light used for irradiation. The changes in the relative populations of **IO1** and **IO2** were more pronounced when irradiation was performed at wavelengths shorter than 312 nm. However, exposure of the matrix to UV ($\lambda \leq 311$ nm) light was inducing (together with **IO1** ↔ **IO2** isomerization) other photoprocesses, which consume the amino–oxo **AO** tautomer.

3.2 Phototautomeric reactions consuming the amino–oxo form

The spectral signatures of minor **IO1** and **IO2** forms, identified on the basis of UV (314–312 nm) irradiation, are all of low or very low intensity. The IR bands due to the significantly more populated **AH1**, **AH2** and **AO** forms are (nearly all) much stronger. The strongest in the whole IR spectrum are the

bands due to **AH1** and **AH2**. As it has been recently reported,⁹ NIR irradiation of matrix-isolated cytosine at 7013 cm^{-1} causes the **AH1** \rightarrow **AH2** rotamerization, whereas NIR irradiation at 7034 cm^{-1} results in the opposite **AH2** \rightarrow **AH1** conversion. Then the spectral changes induced by such NIR irradiations (see Fig. S1a and S2a in the ESI[†]) serve as an effective tool for identification of the bands due to **AH1** and **AH2** forms in the spectrum of matrix-isolated cytosine. The bands assigned in the previous section of the current paper to **IO1** and **IO2** are not affected by NIR irradiation at either 7013 cm^{-1} or 7034 cm^{-1} . Apart from the bands attributed to **IO1** and **IO2**, another set of bands, with the most intense features at 3471 , $1720/1717$, 1656 , 1538 and 1474 cm^{-1} , remained unchanged upon any NIR irradiation (see Fig. S1 and S2 (ESI[†]), traces a and b). These bands are the spectral signatures of the amino-oxo **AO** tautomer.

UV irradiations at 312.0 and at 311.5 nm , similarly to irradiations at longer wavelengths, induced no changes in cytosine molecules adopting the **AO** form. On the other hand, irradiations at shorter wavelengths (starting from 311.2 and 311.0 nm) led to photoprocesses consuming the **AO** form. Upon irradiation at 311 nm , the population of **AO** systematically decreases (see Fig. 2a), as it is indicated by the intensity decrease of the characteristic bands due to **AO** form, e.g. those due to the stretching vibrations of the N1–H and C=O groups (found at 3471 and at $1720/1717\text{ cm}^{-1}$, respectively, see Fig. 3). The decrease of the bands assigned to **AO** is accompanied by increase of many other bands in the IR spectrum (Fig. 2a).

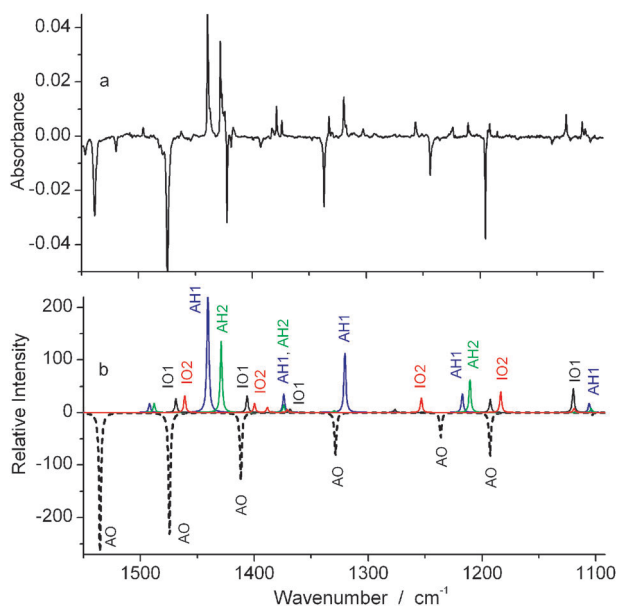


Fig. 2 Phototransformation of the **AO** tautomer of matrix-isolated cytosine into the **AH1**, **AH2**, **IO1** and **IO2** forms. (a) Subtraction result: the experimental spectrum recorded after UV irradiation at 311 nm minus the spectrum recorded after the previous UV irradiation at 312 nm ; (b) the spectra theoretically simulated at the DFT(B3LYP)/6-31++G(d,p) level for **AH1** (blue), **AH2** (green), **IO1** (black solid line), **IO2** (red) and **AO** (black dashed line) isomers of cytosine. Intensities in the theoretical spectra have the following weights: 2 for **AH1**, 1 for **AH2**, 1 for **IO1**, 1 for **IO2** and -5 for **AO**. Theoretical wavenumbers were scaled by 0.978 .

Comparison with the spectra simulated for **AH1**, **AH2**, **IO1** and **IO2** (Fig. 2b) suggests that populations of all of these four isomers increase at the expense of the consumed **AO** form.

As far as the imino-oxo **IO1** and **IO2** forms are concerned, their photostationary ratio obtained after irradiation at 311 nm was, in a good approximation, the same as that obtained after irradiation at 312 nm (Fig. 3). A shift of the wavelength of the exciting UV light by only 1 nm did not noticeably change this photostationary ratio. However, such a small wavelength change had a dramatic effect on the photochemical behavior of **AO** form. Upon irradiation at 312 nm the population of **AO** stayed unchanged, whereas by irradiation at 311 nm this form was quickly consumed and transformed into photoproducts (see the decreasing bands at 3471 , at $1720/1717$ and at 743 cm^{-1} in Fig. 3). Comparison of the two spectra presented in Fig. 3 demonstrates that upon UV ($\lambda = 311\text{ nm}$) irradiation the population decrease of **AO** was accompanied by an increase of population of both imino-oxo **IO1** and **IO2** isomers. It is revealed by the intensity increase of the IR bands at 1757 , 1752 , 1747 and 747 cm^{-1} (all assigned to **IO1**) as well as by the intensity increase of the bands at 1750 and 751 cm^{-1} (assigned to **IO2**). Hence, the total population of the imino-oxo tautomer (in its **IO1** and **IO2** forms) must have increased at the expense of the amino-oxo **AO** tautomer. This proves the occurrence of the amino \rightarrow imino photoisomerization in cytosine monomers isolated in low-temperature environment and excited with UV ($\lambda \leq 311\text{ nm}$) light. The photochemical behavior of the band

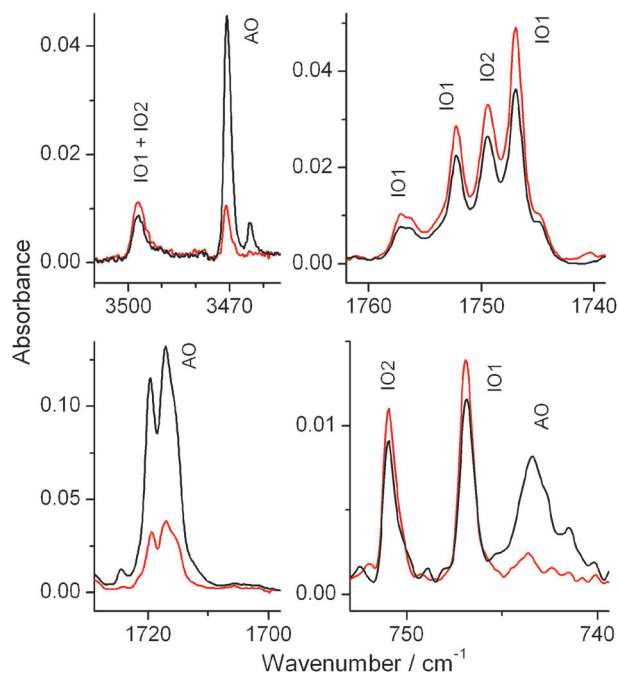


Fig. 3 Spectral indications of the amino \rightarrow imino phototautomeric reaction converting the **AO** tautomer into **IO1** and **IO2** forms. Fragments of the infrared spectrum of cytosine monomers isolated in an Ar matrix: (black) recorded after irradiation of the matrix with UV ($\lambda = 312\text{ nm}$) monochromatic laser light; (red) recorded after subsequent irradiation of the matrix with UV ($\lambda = 311\text{ nm}$) monochromatic laser light. The bands marked as **IO1** and **IO2** were attributed to these forms on the basis of their behavior upon irradiation at 312 nm (see Fig. 1).

observed at 3497 cm^{-1} provides a further support to this conclusion. A counterpart of this band was observed⁸ at 3500 cm^{-1} in the spectrum of cytosine monomers in helium nanodroplets. This absorption was interpreted⁸ as a result of overlapping bands due to the N1H stretching vibrations in both **IO1** and **IO2** forms. According to the theoretical calculations, both bands should be placed at very similar wavenumbers and have very similar absolute intensities. Hence, the increase of the IR absorption at 3497 cm^{-1} (see Fig. 3), in the spectrum of cytosine isolated in an Ar matrix and irradiated with UV ($\lambda = 311\text{ nm}$) light, must reflect increase of the combined populations of **IO1** and **IO2** forms.

UV-induced consumption of **AO** form and the corresponding population increase of the photogenerated products were found to be basically the same for irradiations at any wavelength in the 311–300 nm range. Only the photostationary population ratio of **IO1** and **IO2** showed a non-negligible dependence on the wavelength of the exciting light. Intensity decrease and ultimate disappearance of the bands due to **AO**, occurring upon irradiation at 311–300 nm, allowed an easy identification of the IR spectral features of this form. In the 1800–1000 cm^{-1} range, shown in Fig. 2 and 4, the spectrum of the bands decreasing upon UV ($\lambda = 311\text{--}300\text{ nm}$) irradiation agrees well with the spectrum theoretically predicted for the **AO** tautomer. Population increase of the amino–hydroxy **AH1** and **AH2** forms accompanied consumption of the **AO** tautomer. This oxo \rightarrow hydroxy phototautomerism occurred upon UV irradiation at 311 nm (Fig. 2) as well as upon irradiation at shorter wavelengths down to 300 nm (Fig. 5 and Fig. S1–S3 in the ESI†). All bands due to **AH1** and **AH2** (experimentally identified by the effects of NIR irradiation, Fig. S1 and S2 (ESI†)) increased at the expense of the **AO** reactant. The increasing spectrum included the most characteristic bands

due to OH stretching vibrations, observed at 3601 and 3591 cm^{-1} (see Fig. 5 and Fig. S1 and S3 (ESI†)). In the previous studies of Szczesniak *et al.*,¹⁰ where cytosine was irradiated at much shorter wavelengths ($\lambda > 250\text{ nm}$), no growth but small decrease of the bands due to the amino–hydroxy tautomer was reported, with simultaneous significant reduction of the intensity of the bands due to the amino–oxo form.

The photoeffects described above allowed attribution of the bands observed in the IR spectrum to particular forms of cytosine. The complete list of assignments of the IR absorption bands of matrix-isolated cytosine monomers to the spectra of **AO**, **AH1**, **AH2**, **IO1** and **IO2** isomers is provided in Table S1 in the ESI† (see also Fig. S1, S2 and S4 in the ESI†).

Population increase of **AH1**, **AH2**, **IO1** and **IO2** forms, occurring (upon irradiations at 311–300 nm) at the expense of the decreasing population of **AO** (see Fig. 2, 3 and 5 and Fig. S1–S3 in the ESI†), does not mean that all the four isomers are primary photoproducts generated directly from the **AO** reactant. Most probably, the UV-induced oxo \rightarrow hydroxy and amino \rightarrow imino hydrogen-atom-transfer processes generate **AH1** and **IO1** as primary products (see Scheme 3). Forms **AH1** and **IO1** can then be partially converted into their **AH2** and **IO2** counterparts. The **AH1** \leftrightarrow **AH2** equilibrium can be achieved during vibrational relaxation following the UV-induced hydrogen-atom transfer. It can be also induced by exposure of the matrix to NIR radiation of the spectrometer source. As described in the previous section, UV excitation, causing the *syn* \leftrightarrow *anti* isomerization, should be the driving force of the **IO1** \leftrightarrow **IO2** photoequilibrium. In such a manner, as shown in Scheme 3, forms **AH2** and **IO2** are also populated, though not directly, at the expense of the decreasing population of **AO**.

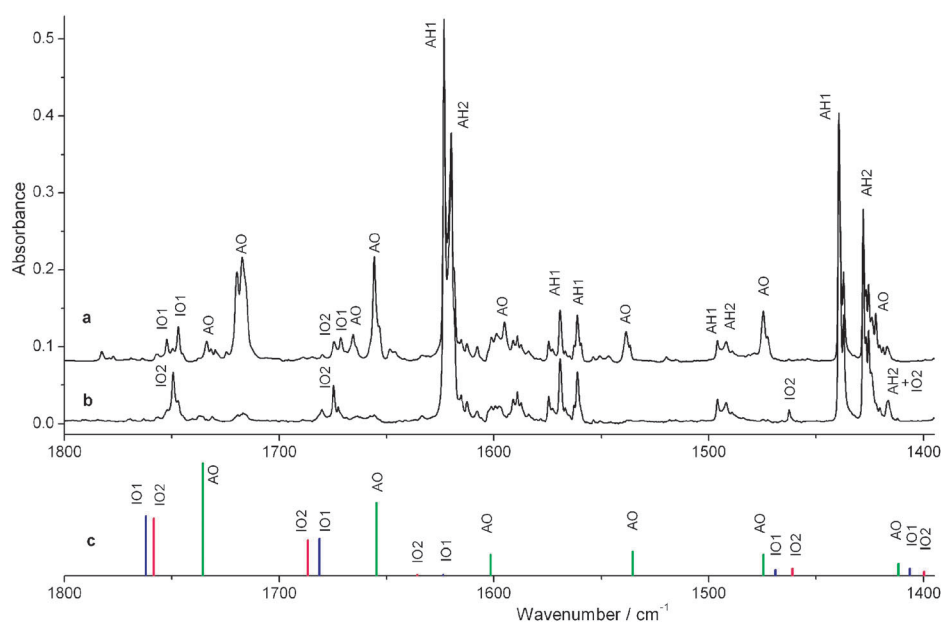


Fig. 4 Fragments of the infrared spectrum of cytosine monomers isolated in an Ar matrix: (a) recorded after deposition of the matrix; (b) recorded after irradiation of the matrix with UV ($\lambda = 300\text{ nm}$) monochromatic laser light; (c) calculated at the DFT(B3LYP)/6-31++G(d,p) level for: (green) **AO**, (blue) **IO1** and (magenta) **IO2** forms of cytosine. In the theoretical spectra wavenumbers were scaled by 0.978, and intensities of **IO1** and **IO2** were scaled by 0.5. The bands marked as **AH1** and **AH2** were attributed to these forms on the basis of their behavior upon NIR irradiations at 7034 cm^{-1} and at 7013 cm^{-1} (see ref. 9 and Fig. S2 in the ESI†).

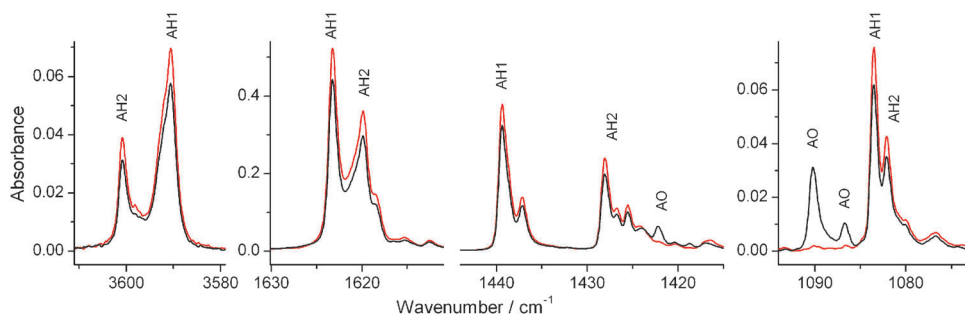
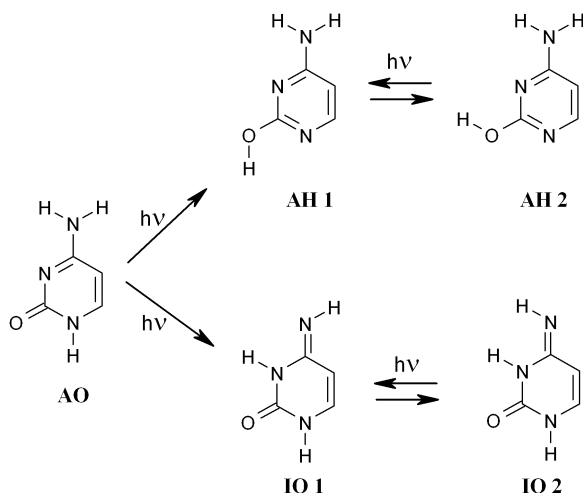


Fig. 5 Spectral indications of the oxo \rightarrow hydroxy phototautomeric reaction converting the **AO** tautomer into **AH1** and **AH2** forms. Fragments of the infrared spectrum of cytosine monomers isolated in an Ar matrix: (black) recorded after deposition of the matrix; (red) recorded after irradiation of the matrix with UV ($\lambda = 300$ nm) monochromatic laser light. The bands marked as **AH1** and **AH2** were attributed to these forms on the basis of their behavior upon NIR irradiations at 7034 cm^{-1} and at 7013 cm^{-1} (see ref. 9 and Fig. S1 and S2 in the ESI †).



Scheme 3 UV-induced hydrogen-atom-transfer processes converting the amino-oxo tautomer of cytosine into the amino-hydroxy and imino-oxo forms.

3.3 More on the *syn* \leftrightarrow *anti* photoisomerization in the imino-oxo forms

Upon irradiations of the matrix at wavelengths shorter than 311 nm, the population ratio of **IO1** and **IO2** was changing. The relative population of **IO2** increased upon decreasing the wavelength of the exciting UV light. At the photostationary state resulting after irradiation at 300 nm (Fig. 6, red trace, see also Fig. S5 in the ESI †), nearly all the population of the imino-oxo tautomer was converted into **IO2**.

Following the irradiation at 300 nm, the matrix was exposed again to longer-wavelength UV ($\lambda = 311$ nm) light. This last irradiation shifted the ratio of **IO1** and **IO2** to a state with higher population of **IO1** and lower population of **IO2**, with respect to the photoequilibrium previously induced by irradiation at 300 nm (see Fig. 6, blue trace). Observation of the partial repopulation of the **IO1** isomer, nearly totally consumed by the previous shorter-wavelength irradiation, provides a direct proof of the photoreversibility of the *syn* \leftrightarrow *anti* photoisomerization involving the two imino-oxo forms of cytosine.

A difference spectrum, obtained by subtraction of the spectrum recorded after 300 nm irradiation from the spectrum recorded after the subsequent irradiation at 311 nm, is presented

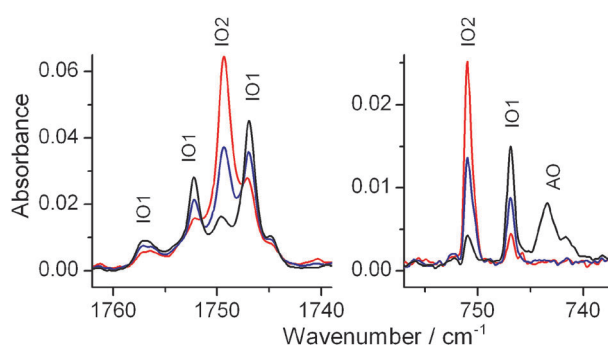


Fig. 6 Photostationary states of the **IO1** \leftrightarrow **IO2** conversion as a function of the wavelength of exciting UV light. Fragments of the infrared spectrum of cytosine monomers isolated in an Ar matrix: (black) recorded after deposition of the matrix; (red) recorded after irradiation of the matrix with UV ($\lambda = 300$ nm) monochromatic laser light; (blue) recorded after subsequent irradiation of the matrix with UV ($\lambda = 311$ nm) monochromatic laser light.

in Fig. 7. Since the 300 nm irradiation led to total consumption of **AO** (see Fig. 4–6 and Fig. S1 and S2 in the ESI †) and since **AH1** and **AH2** do not absorb UV light at either 300 nm or 311 nm, the spectral changes induced by the last 311 nm irradiation must concern only the **IO1** and **IO2** imino-oxo isomers. The spectrum of the bands increasing upon the last irradiation at 311 nm and the spectrum of the bands decreasing upon this irradiation are compared (in Fig. 7) with the spectra theoretically simulated for **IO1** and **IO2**. The good agreement between the experimental and theoretical spectra supports the correctness of the assignment of these two sets of bands to **IO1** and **IO2**. Moreover, this comparison supports the assignment of the imino-oxo form more populated in the matrix before any irradiation to **IO1**, as well as the assignment of the form being only very slightly populated just after deposition of the matrix to **IO2**. Such interpretation fully agrees with the theoretical predictions of the relative energies of the isomeric forms of cytosine.^{5,16}

3.4 Minor photoreactions

The main photoeffect observed upon UV irradiation of matrix-isolated cytosine concerned the photoreactions consuming **AO** tautomeric form. There is no doubt that the majority of **AO**

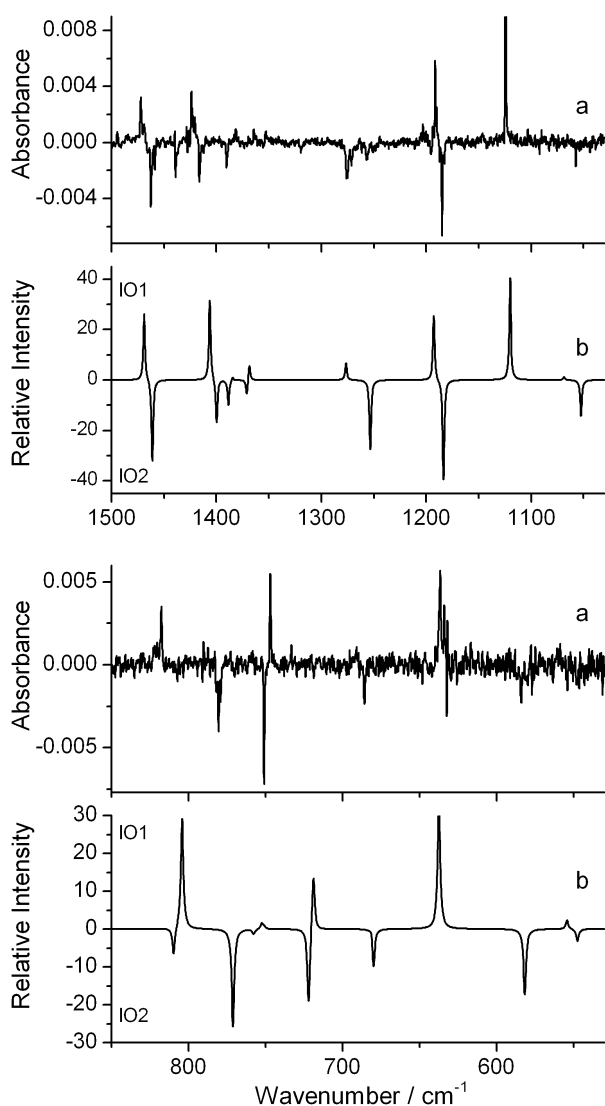


Fig. 7 Identification of **IO1** and **IO2** imino-oxo isomers of cytosine: (a) difference spectrum, obtained by subtraction of the spectrum recorded after UV ($\lambda = 300$ nm) irradiation from the spectrum recorded after the subsequent UV ($\lambda = 311$ nm) irradiation; (b) subtraction result: the spectrum theoretically simulated for the **IO1** form minus the spectrum simulated for **IO2**. Theoretical spectra were calculated at the DFT(B3LYP)//6-31++G(d,p) level and the theoretical wavenumbers were scaled by 0.978.

population was transformed, by the oxo \rightarrow hydroxy and amino \rightarrow imino phototautomeric reactions, into **AH** and **IO** tautomers. However, irradiation of the matrix with UV ($\lambda = 311$ – 300 nm) light, causing decrease of the population of the **AO** reactant, led also to the appearance of a structured IR absorption at 2300 – 2230 cm⁻¹ (Fig. 8). The main component of this complex band was found at 2266 cm⁻¹. Most probably, this band indicates that an open-ring isocyanate product was generated in an α -bond cleavage photoreaction. Analogous processes were previously observed for matrix-isolated 1-methylcytosine and the model compound 1-methyl-2(1*H*)-pyrimidinone.¹⁸ The structures of these compounds are very similar to that of the **AO** tautomer of cytosine. For 1-methylcytosine and for 1-methyl-2(1*H*)-pyrimidinone, UV irradiation caused generation

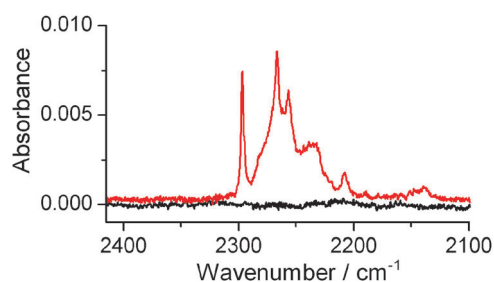


Fig. 8 Fragment of the infrared spectrum of cytosine monomers isolated in an Ar matrix: (black) recorded after deposition of the matrix; (red) recorded after irradiation of the matrix with UV ($\lambda = 300$ nm) monochromatic laser light.

of photoproducts characterized by strong, structured IR absorptions centered at 2261 and 2262 cm⁻¹, respectively. Such frequency and high intensity is typical of bands due to the “antisymmetric” stretching vibration of the $-\text{N}=\text{C}=\text{O}$ isocyanate group. For instance, in the IR spectrum of methylisocyanate,¹⁹ a very intense, complex absorption (with a principal component at 2289 cm⁻¹) was observed in the 2360 – 2235 cm⁻¹ region. Detailed analysis, carried out for the photoproduct generated upon UV irradiation of 1-methyl-2(1*H*)-pyrimidinone,¹⁸ confirmed the open-ring, conjugated isocyanate structure of this species. Hence, it looks quite likely that also for the **AO** isomer of cytosine, UV excitation generates the open-ring isocyanate as a minor photoproduct. The amount of this product photogenerated from cytosine must be really tiny, because the observed intensity of the spectral signature at *ca.* 2266 cm⁻¹ was low and absolute intensities of IR bands due to “antisymmetric” stretching vibrations of the $-\text{N}=\text{C}=\text{O}$ isocyanate groups are very high,^{18,19} usually higher than 1000 km mol⁻¹.

3.5 Remarks on the mechanisms of the observed photoisomerizations

The *syn* \leftrightarrow *anti* photoisomerization, observed for **IO1** and **IO2** forms of cytosine, belongs to the known category of photoinduced rotations around C=N double bonds. The mechanism of such photoisomerization is similar to that of the photoinduced *cis* \leftrightarrow *trans* rotation around C=C double bonds. In such photoreactions, the key role is played by a low-energy conical intersection between S_1 and S_0 , placed at a structure with the substituent group (attached to C=N) rotated by *ca.* 90° , with respect to the ground-state minima of the *syn* and *anti* forms.^{20,21} The shapes of the potential energy surfaces of S_1 and S_0 determine the typical photochemical behavior of the compounds with C=N groups. Upon UV excitation, such compounds undergo a *syn* \leftrightarrow *anti* photoisomerization leading to a photostationary state. The relative populations of *syn* and *anti* isomers at a photostationary state are the function of a wavelength of UV light used for excitation.²¹ Then, the photochemical behavior, observed in the current work for **IO1** and **IO2** isomers of cytosine, follows the typical characteristics of *syn* \leftrightarrow *anti* photoisomerizations in compounds with exocyclic C=N groups: (i) UV irradiation led to conversion of **IO1** and **IO2**

forms into each other; (ii) prolonged irradiation at each excitation wavelength was leading to a photostationary state; (iii) at each of the observed photostationary states, the population ratio of **IO1** and **IO2** was a function of the applied UV wavelength.

The phototransformation of the amino–oxo **AO** form into the amino–hydroxy **AH** tautomer is similar to the oxo \rightarrow hydroxy phototautomerism, previously observed for matrix-isolated heterocyclic compounds such as 4(3*H*)-pyrimidinone or 2(1*H*)-pyridinone.²² Photoinduced dissociation of the N–H bond, on the hypersurface of a repulsive $\pi\sigma^*$ state, was proposed to be a key step of the PIDA (PhotoInduced Dissociation Association) mechanism of such phototautomeric reactions.²³ Hence, the oxo \rightarrow hydroxy phototautomerism in isolated heterocyclic molecules may be treated as a case example of photochemistry on surfaces of dissociative $\pi\sigma^*$ states.²⁴ The **AO** \rightarrow **AH** phototransformation in cytosine seems to belong to this class of UV-induced processes.

Also the amino \rightarrow imino phototautomeric reaction converting **AO** form into the **IO** tautomer can be treated as a photoinduced dissociation–association (PIDA) process. Recent experiments, carried out by King *et al.*,²⁵ demonstrated that a hydrogen atom of the NH₂ group in UV-excited aniline dissociates on the potential energy surface of a repulsive $\pi\sigma^*$ state. Most probably, processes of this type are responsible for the amino \rightarrow imino phototautomerism found by Akai *et al.*²⁶ in matrix-isolated 2-aminopyridine and its methylated derivatives. By analogy, it looks very likely that the **AO** \rightarrow **IO** phototransformation in cytosine is also governed by the PIDA mechanism, involving a key role of dissociative $\pi\sigma^*$ states.

4. Conclusions

Experiments on cytosine monomers isolated in Ar matrices and irradiated with monochromatic UV laser light allowed identification of the amino–hydroxy, amino–oxo, and two imino–oxo isomers of the compound. The two imino–oxo forms of cytosine were unambiguously experimentally observed for the first time. These results were combined with separation of the IR spectral signatures of the two amino–hydroxy conformers, possible thanks to the effect of monochromatic NIR irradiation of matrix-isolated cytosine. Altogether, five isomeric forms were experimentally found for cytosine monomers trapped in low-temperature matrices. Four different photoinduced transformations of isomeric forms of cytosine were observed (Scheme 3): (i) UV-induced *syn* \leftrightarrow *anti* mutual isomerizations of the two imino–oxo forms; (ii) NIR-induced conformational isomerization of the two amino–hydroxy forms; (iii) UV-induced oxo \rightarrow hydroxy phototautomeric reaction; (iv) UV-induced amino \rightarrow imino phototautomeric reaction. Photoreactions (i), (iii) and (iv) were induced by irradiation of cytosine monomers with 314–300 nm UV light. Besides providing experimental proofs of the presence of all five isomers of cytosine in low-temperature matrices, the observed photoreactions allowed also a reliable assignment of the IR bands observed in the experimentally recorded spectra to particular isomeric forms of cytosine.

Acknowledgements

The research leading to these results has received funding from the European Community's Seventh Framework Programme under grant agreement no 228334.

References

- 1 C. Canuel, M. Mons, F. Piuze, B. Tardivel, I. Dimicoli and M. Elhanine, *J. Chem. Phys.*, 2005, **122**, 074316.
- 2 H. Kang, K. T. Lee, B. Jung, Y. J. Ko and S. K. Kim, *J. Am. Chem. Soc.*, 2002, **124**, 12958–12959; S. Ullrich, T. Schultz, M. Z. Zgierski and A. Stolow, *Phys. Chem. Chem. Phys.*, 2004, **6**, 2796–2801; K. Kosma, Ch. Schröter, E. Samoylova, I. V. Hertel and T. Schultz, *J. Am. Chem. Soc.*, 2009, **131**, 16939–16943; T. Gustavsson, R. Improta and D. Markovitsi, *J. Phys. Chem. Lett.*, 2010, **1**, 2025–2030.
- 3 H. R. Hudock and T. J. Martínez, *ChemPhysChem*, 2008, **9**, 2486–2490; M. Merchán and L. Serrano-Andrés, *J. Am. Chem. Soc.*, 2003, **125**, 8108–8109; N. Ismail, L. Blancafort, M. Olivucci, B. Kohler and M. A. Robb, *J. Am. Chem. Soc.*, 2002, **124**, 6818–6819; L. Blancafort and M. A. Robb, *J. Phys. Chem. A*, 2004, **108**, 10609–10614.
- 4 G. Fogarasi, *J. Phys. Chem. A*, 2002, **106**, 1381–1390; M. Piacenza and S. Grimme, *J. Comput. Chem.*, 2004, **25**, 83–98; J. K. Wolken, Ch. Yao, F. Tureček, M. J. Polce and Ch. Wesdemiotis, *Int. J. Mass Spectrom.*, 2007, **267**, 30–42.
- 5 S. A. Trygubenko, T. V. Bogdan, M. Rueda, M. Orozco, F. J. Luque, J. Šponer, P. Slaviček and P. Hobza, *Phys. Chem. Chem. Phys.*, 2002, **4**, 4192–4203; R. Kobayashi, *J. Phys. Chem.*, 1998, **102**, 10813–10817.
- 6 R. D. Brown, P. D. Godfrey, D. McNaughton and A. P. Pierlot, *J. Am. Chem. Soc.*, 1989, **111**, 2308–2310.
- 7 V. Feyer, O. Plekan, R. Richter, M. Coreno, G. Vall-llosera, K. C. Prince, A. B. Trofimov, I. L. Zaytseva, T. E. Moskovskaya, E. V. Gromov and J. Schirmer, *J. Phys. Chem. A*, 2009, **113**, 5736–5742.
- 8 M. Y. Choi, F. Dong and R. E. Miller, *Philos. Trans. R. Soc. London, Ser. A*, 2005, **363**, 393–413.
- 9 L. Lapinski, M. J. Nowak, I. Reva, H. Rostkowska and R. Fausto, *Phys. Chem. Chem. Phys.*, 2010, **12**, 9615–9618.
- 10 M. Szczesniak, K. Szczepaniak, J. S. Kwiatkowski, K. KuBulat and W. B. Person, *J. Am. Chem. Soc.*, 1988, **110**, 8319–8330; M. J. Nowak, L. Lapinski and J. Fulara, *Spectrochim. Acta, Part A*, 1989, **45**, 229–242.
- 11 L. Lapinski, M. J. Nowak, J. Fulara, A. Leś and L. Adamowicz, *J. Phys. Chem.*, 1990, **94**, 6555–6564.
- 12 A. D. Becke, *Phys. Rev. A*, 1988, **38**, 3098–3100.
- 13 C. T. Lee, W. T. Yang and R. G. Parr, *Phys. Rev. B: Condens. Matter*, 1988, **37**, 785–789.
- 14 M. J. Frisch, G. W. Trucks, H. B. Schlegel, G. E. Scuseria, M. A. Robb, J. R. Cheeseman, J. A. Montgomery, Jr, T. Vreven, K. N. Kudin, J. C. Burant, J. M. Millam, S. S. Iyengar, J. Tomasi, V. Barone, B. Mennucci, M. Cossi, G. Scalmani, N. Rega, G. A. Petersson, H. Nakatsuji, M. Hada, M. Ehara, K. Toyota, R. Fukuda, J. Hasegawa, M. Ishida, T. Nakajima, Y. Honda, O. Kitao, H. Nakai, M. Klene, X. Li, J. E. Knox, H. P. Hratchian, J. B. Cross, V. Bakken, C. Adamo, J. Jaramillo, R. Gomperts, R. E. Stratmann, O. Yazyev, A. J. Austin, R. Cammi, C. Pomelli, J. W. Ochterski, P. Y. Ayala, K. Morokuma, G. A. Voth, P. Salvador, J. J. Dannenberg, V. G. Zakrzewski, S. Dapprich, A. D. Daniels, M. C. Strain, O. Farkas, D. K. Malick, A. D. Rabuck, K. Raghavachari, J. B. Foresman, J. V. Ortiz, Q. Cui, A. G. Baboul, S. Clifford, J. Cioslowski, B. B. Stefanov, G. Liu, A. Liashenko, P. Piskorz, I. Komaromi, R. L. Martin, D. J. Fox, T. Keith, M. A. Al-Laham, C. Y. Peng, A. Nanayakkara, M. Challacombe, P. M. W. Gill, B. Johnson, W. Chen, M. W. Wong, C. Gonzalez and J. A. Pople, *Gaussian 03*, Gaussian, Inc., Wallingford CT, 2004.
- 15 E. Nir, Ch. Plützer, K. Kleinermanns and M. de Vries, *Eur. Phys. J. D*, 2002, **20**, 317–329; E. Nir, M. Müller, L. I. Grace and M. S. de Vries, *Chem. Phys. Lett.*, 2002, **355**, 59–64.

- 16 G. Fogarasi, *J. Mol. Struct.*, 1997, **413**, 271–278.
- 17 M. Szczesniak, J. Leszczynski and W. B. Person, *J. Am. Chem. Soc.*, 1992, **114**, 2731–2733.
- 18 L. Lapinski, H. Rostkowska, A. Khvorostov, R. Fausto and M. J. Nowak, *J. Phys. Chem. A*, 2003, **107**, 5913–5919.
- 19 I. Reva, L. Lapinski and R. Fausto, *J. Mol. Struct.*, 2010, **976**, 333–341.
- 20 D. S. Ruiz, A. Cembran, M. Garavelli, M. Olivucci and W. Fuss, *Photochem. Photobiol.*, 2002, **76**, 622–633.
- 21 L. Lapinski, M. J. Nowak, A. L. Sobolewski and B. Kierdaszuk, *J. Phys. Chem. A*, 2006, **110**, 5038–5046.
- 22 M. J. Nowak, J. Fulara and L. Lapinski, *J. Mol. Struct.*, 1988, **175**, 91–96; L. Lapinski, M. J. Nowak, A. Les and L. Adamowicz, *J. Am. Chem. Soc.*, 1994, **116**, 1461–1467; A. Gerega, L. Lapinski, M. J. Nowak, A. Furmanchuk and J. Leszczynski, *J. Phys. Chem. A*, 2007, **111**, 4934–4943.
- 23 B. Chmura, M. F. Rode, A. L. Sobolewski, L. Lapinski and M. J. Nowak, *J. Phys. Chem. A*, 2008, **112**, 13655–13661.
- 24 M. N. R. Ashfold, G. A. King, D. Murdock, M. G. D. Nix, T. A. A. Oliver and A. G. Sage, *Phys. Chem. Chem. Phys.*, 2010, **12**, 1218–1238; A. L. Sobolewski, W. Domcke, C. Dedonder-Lardeux and C. Jouvet, *Phys. Chem. Chem. Phys.*, 2002, **4**, 1093–1100.
- 25 G. A. King, T. A. A. Oliver and M. N. R. Ashfold, *J. Chem. Phys.*, 2010, **132**, 214307.
- 26 N. Akai, K. Ohno and M. Aida, *Chem. Phys. Lett.*, 2005, **413**, 306–310; N. Akai, T. Harada, K. Shin-ya, K. Ohno and M. Aida, *J. Phys. Chem. A*, 2006, **110**, 6016–6022; N. Akai, K. Ohno and M. Aida, *J. Photochem. Photobiol., A*, 2007, **187**, 113–118.